Pyridine Adsorption and Acid/Base Complex Formation on Ultrathin Films of γ-Al_2O_3 on NiAl(100)

Kathryn A. Layman, Michelle M. Ivey, and John C. Hemminger*

Department of Chemistry and Institute for Surface and Interface Science, University of California, Irvine, Irvine, California 92697

Received: January 13, 2003; In Final Form: May 21, 2003

Pyridine adsorption on NiAl(100) and ultrathin films of γ-Al_2O_3 was studied using high-resolution electron energy loss spectroscopy (HREELS). Pyridine adsorbs on NiAl(100) with its molecular axis parallel to the surface plane at low coverages and with its molecular plane inclined more toward the surface normal at higher coverages. On the hydroxylated and nonhydroxylated thin films of γ-Al_2O_3, pyridine interacts with the coordinatively unsaturated Al^{3+} cations via its nitrogen lone-pair electrons. Pyridine was also found to interact with the surface hydroxyl groups on the hydroxylated γ-Al_2O_3 thin films, forming C_5H_5N−HO complexes. Complex formation causes the OH bond strength to decrease and the OH stretch vibration to shift from 3711 cm^{-1}, which is characteristic of uncomplexed, isolated OH, to lower frequency. At low coverages, pyridine only interacts with the more acidic surface OH groups, those located on 3-fold Al^{3+} cation sites. This interaction forms a C_5H_5N−HO complex, which has an O−H stretch at 2920 cm^{-1}. As the coverage is increased, an additional C_5H_5N−HO complex is formed from an interaction between pyridine and the less acidic OH groups, which are bonded to 2 Al^{3+} cations. The vibrational frequency for O−H stretch of this C_5H_5N−HO complex is 3150 cm^{-1}. As the intensities for the O−H stretches of the C_5H_5N−HO complexes increase, the intensity for the free O−H stretch at 3711 cm^{-1} decreases. The interaction with the surface hydroxyl groups is reversible, confirming that the observed shifts in the O−H stretching frequency result from the formation of weakly bonded acid−base complexes. While most of the pyridine desorbs from the γ-Al_2O_3 thin films by 290 K, annealing the pyridine-dosed γ-Al_2O_3 thin films to temperatures above 290 K, results in a small amount of pyridine dehydrogenation and the formation of surface OH groups with an O−H stretch at 3742 cm^{-1}.

1. Introduction

Aluminum oxide (Al_2O_3) is used as an industrial acid−base catalyst[1−6] and metallic catalyst support.[7−9] Al_2O_3 is also a major component of mineral dust and solid fuel rocket exhaust. As a result of its catalytic properties and abundance in the atmosphere, Al_2O_3 may have an important role in the processing of air pollutants.

A detailed understanding of the catalytic properties of Al_2O_3 is lacking because of the structural and chemical complexity of powdered Al_2O_3, such as the quantity and acidity of the available Lewis acid and Brønsted acid sites. Al_2O_3 can exist in several phases, all of which consist of a close-packed oxygen lattice in which the aluminum cations occupy the tetrahedral and/or octahedral vacancies. In α-Al_2O_3, the most stable phase, the aluminum cations occupy only the octahedral vacancies in a hexagonal closest-packed oxygen sub-lattice. In contrast, in the metastable γ phase of Al_2O_3, the aluminum cations occupy both the tetrahedral and octahedral vacancies in a face-centered-cubic oxygen sub-lattice.[10−12] γ-Al_2O_3, the more reactive form of alumina, is used extensively as a catalyst[1−6] and a catalyst support.[7−9] However, because γ-Al_2O_3 exists only in powdered form, the exposed faces, and thus available Lewis acid sites, vary from experiment to experiment.

Further complexity is added by the variable degree of hydroxylation that exists on the Al_2O_3 surface due to changes in humidity and pretreatment conditions. Water readily adsorbs to the surface as molecular water or dissociates to form hydroxyl groups on the Al_2O_3 surface. The hydroxyl groups can occupy a variety of sites on the Al_2O_3 surface. The adsorption site and number of neighboring hydroxyl groups influence the acidity and the OH vibrational stretch frequency of each type of hydroxyl group.[4,13−15] On the basis of their work on powdered samples, Knözinger and Ratnasamy have assigned the complex OH stretch observed in most IR spectra of Al_2O_3 to be due to the presence of 5 different types of isolated hydroxyl groups, in addition to associated hydroxyl groups and molecular water.[4] The processing of most Al_2O_3 catalysts involves annealing to higher temperatures prior to use in order to remove the water and surface hydroxyl groups. The removal of the surface hydroxyl groups increases the Al_2O_3 catalytic activity by increasing the number of surface defect sites, which are predominantly coordinatively unsaturated Al^{3+} cations adjacent to anionic vacancies.

By growing ultrathin films of Al_2O_3 ($\leq$ 20 Å thick) on conducting substrates, the surface potential of the insulator is stabilized,[16] facilitating the use of surface specific probes. Consequently, significant research has been devoted to the development of oxide film growth recipes to create structurally and chemically well-defined Al_2O_3 surfaces which mimic the more complex powdered samples of γ-Al_2O_3, and which can be studied using modern surface spectroscopy to obtain information about the surface structure, elemental composition, and

* Corresponding author. E-mail: jchemmin@uci.edu.

10.1021/jp030046p CCC: $25.00
Published on Web 07/19/2003

surface vibrational spectroscopy. While there are several methods for growing thin films of Al_2O_3 on conducting substrates,[16−31] we have chosen to grow our γ-like Al_2O_3 thin films on NiAl(100). By adapting the method of Gassmann et al.[11,26] we have learned to generate highly ordered Al_2O_3 ultrathin films with well-defined structure on NiAl(100). We were the first to show that well-defined Al_2O_3 ultrathin films can be grown with surface OH groups on NiAl(100).[32,33] Thus, we are able to grow both nonhydroxylated and hydroxylated thin films of γ-like Al_2O_3. The only difference in the vibrational spectra of the nonhydroxylated and hydroxylated γ-like Al_2O_3 films is that the hydroxylated films have a single OH stretch at $\sim$3711 cm^{-1}. This frequency is indicative of isolated, noninteracting, hydroxyls (OH groups).[4,34] Based on the assignments of Knözinger and Ratnasamy, we can tell that we are only generating surface OH groups that are bonded to either 2 or 3 Al^{3+} sites, as shown schematically below. The vibrational

spectrum of the hydroxylated γ-like Al_2O_3 thin film is much less complicated than the vibrational spectrum of powdered γ-Al_2O_3, which has a very broad (500 cm^{-1}) OH spectrum.

As has been observed for powdered samples of alumina, the chemistry of the γ-like Al_2O_3 thin films is affected by the surface composition, particularly the quantity, types, and acidity of the surface catalytic sites.[13,14,35] Perhaps, the most important sites are the surface hydroxyl groups because they provide the sites for Brønsted acid-catalyzed reactivity, as we have reported for the dimerization of 1,3-butadiene on hydroxylated thin films of γ-like Al_2O_3.[32,33] Finally, Heemeier et al. have shown that increasing the concentration of surface hydroxyl groups increases metal dispersion on metallic supported catalysts,[36] presumably due to the addition of more nucleation sites for metal particle growth.

Many techniques have been developed to quantify surface acidity. Of these methods, analytical methods that study the adsorption of basic probe molecules on metal oxide surfaces are the most widely employed. In these experiments, the probe molecule, P, interacts with a catalytic site, S, given by the following equilibrium:

$$P + S \rightleftarrows P{-}S$$

where P−S may be a coordination surface compound, a surface complex ion, or a charge transfer complex. This method, known as specific poisoning, requires that the probe molecule interacts only with the specific active sites being investigated.[13,14,35] Because metal oxides have several catalytic sites, including Brønsted acid, Lewis acid, and Lewis base sites, the characterization of surface acidity is often complex. In general, a whole set of probe molecules of various properties is needed in order to gain a detailed understanding of the various types of acid sites available on the metal oxide surface.[13,14,35]

The best results for determining the total acidity of metal oxides are obtained by adsorbing pyridine onto the oxide surface.[14,37] On weak basic systems, pyridine does not undergo surface reactions until very high temperatures.[14] In addition, the frequencies and intensities of some of the pyridine ring vibrations are highly sensitive to the nature of the pyridine interaction with an adsorption site via the nitrogen-lone-pair electrons.[13,14,35,37−40] Thus, vibrational spectroscopy can be used to distinguish between pyridine interacting with coordinatively unsaturated metal cations (Lewis acid sites), with Brønsted acid sites, forming a pyridium ion, or with weak surface hydroxyl groups, to which pyridine forms a hydrogen bond. These interactions are depicted schematically in Figure 1.

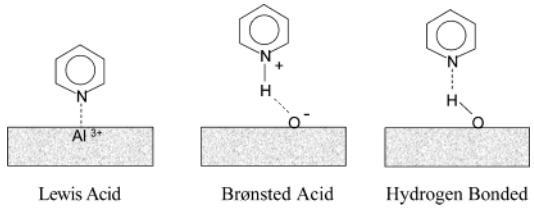

Figure 1. Schematic for pyridine interacting with (a) Lewis acid, (b) Brønsted acid, and (c) weak surface OH sites on metal oxide surfaces.

Using the nomenclature of Wilson,[41] the most sensitive IR-active vibrations are υ_{8a}, υ_{8b}, υ_{19a}, and υ_{19b}. In Raman spectroscopy, the ring breathing region (υ_1 and υ_{12}) is used, since the vibrations used in IR spectroscopy are weak. While the shifts and relative intensities of the ring vibrations may depend on the nature of the catalyst, the general positions of the ring vibrations of pyridine interacting with a given type of adsorption site has been determined from model systems and are listed in Table 1. In general, the band around 1540 cm^{-1} is assumed to be characteristic of pyridium ions, while bands between 1445 and 1464 cm^{-1} are attributed to coordinatively adsorbed pyridine.[13,14,35,37,38,40,42]

The vibrations of adsorbed pyridine do not distinguish the acidity of surface hydroxyl groups acting as Brønsted acid sites because the band at 1540 cm^{-1} does not change in wavenumber upon varying the acidity of the solid.[13,35,38] However, the pyridine vibrational spectrum can be used to distinguish the acidity of various Lewis acid sites since the frequency of the band indicative of coordinatively bonded pyridine increases as the interaction strength increases.[14,35,38] In general, the coordinatively unsaturated metal cations with tetrahedral coordination interact more strongly with pyridine than the coordinatively unsaturated metal cations in the octahedral holes. For metal cations with the same coordination geometry, the strength of interaction increases as the ratio of the formal charge to the radius of the metal cation increases.[35]

We show in this paper that vibrational spectroscopy coupled with pyridine adsorption can distinguish between surface hydroxyl groups to which it associates, by hydrogen-bond formation. This is accomplished by following the O−H stretch vibrational frequency as opposed to the pyridine vibrations.

2. Experimental Section

The HREELS experiments were carried out in an ion-pumped UHV chamber that has a base pressure of $\sim 1 \times 10^{-10}$ Torr. The chamber is equipped with a single-pass cylindrical mirror analyzer (Physical Electronics 10-155) with a coaxial electron gun for Auger electron spectroscopy (AES) analysis, an UTI-100C quadrupole mass spectrometer for residual gas analysis, Varian low-energy electron diffraction (LEED) optics, an LK-2000 high-resolution electron energy loss spectrometer (HREELS), and an ion gun for ion bombardment.

Typical HREELS conditions were the following: incident electron beam with kinetic energy in the range of 5−7 eV, resolution of $\sim$5−8 meV, and count rates $\sim$100 kHz in the elastic, and 1−10 kHz in inelastic channels. All HREEL spectra presented here were recorded at a substrate temperature $\leq$170 K. The period of signal averaging was kept at $\sim$2 h per spectrum in order to maximize the signal-to-noise ratio. Each HREELS

TABLE 1: Vibrational Frequencies of Pyridine Used in Characterization of Metal Oxide Surfaces (based on model systems)

mode	symmetry	liquid[a]	gas phase[b]	hydrogen-bonded[a]	Brönsted acid[a]	Lewis acid[a]
$\bar{\upsilon}_{8a}$	A_1	1582	1583	1590−1600	1640	1600−1633
$\bar{\upsilon}_{8b}$	B_2	1575	1572	1580−1590	1620	1580
$\bar{\upsilon}_{19a}$	A_1	1482	1482	1485−1490	1485−1500	1488−1503
$\bar{\upsilon}_{19b}$	B_2	1438	1439	1440−1447	1540	1447−1460
$\bar{\upsilon}_{12}$	A_1	1031	1030	1032−1040	1024−1035	1040−1050
$\bar{\upsilon}_{1}$	A_1	991	981	996−1005	1007−1015	1016−1028

[a] Ref 38. [b] Refs 69 and 81.

spectrum, unless otherwise noted, was normalized with respect to its own elastic peak and the corresponding number of scans.

The laser-induced thermal desorption (LITD-FTMS) experiments were carried out in a separate ion-pumped UHV chamber with a base pressure of $\sim 5 \times 10^{-10}$ Torr. The chamber is equipped with a single-pass cylindrical mirror analyzer (Physical Electronics 10-155) equipped with an electron gun for AES analysis, PHI LEED optics, and an ion gun for ion bombardment. The LITD-FTMS experimental details have been described in our previous publications.[32,43−68] Briefly, in a typical LITD-FTMS experiment, a 0.5 mm × 1 mm spot is irradiated with a pulsed laser (KrF eximer laser, 248 nm, 20 ns pulse width). The resultant rapid temperature jump causes the intact desorption of molecular adsorbates, even if slower heating rates would have resulted in a surface reaction.[52,54,62,69] The neutral molecules are then ionized by electron ionization (70 eV) and detected by Fourier transform mass spectrometry (FTMS).[54] The laser optics are controlled such that each laser pulse probes a different spot on the surface. The use of FTMS to detect and identify the laser-desorbed species provides a complete mass spectrum from each laser pulse incident on the surface, with very good sensitivity.

NiAl(100) samples were prepared from a 1 cm diameter single crystal rod of NiAl, obtained from GE Research Labs (Schnectady, New York). After cutting 2 mm thick slices from the rod using an electric discharge machine (California Wire EDM), both sides of the crystal were polished using standard procedures. Angular alignment of the NiAl(100) surface was determined by Laue X-ray diffraction. Sample preparation and mounting in the two UHV chambers was essentially identical. The sample was mounted on a liquid nitrogen-cooled manipulator, equipped with resistive heating. A chromel/alumel thermocouple was spot welded to the side of the crystal. Initially, the sample was subjected to room-temperature Ar^+ sputtering for 5 min, followed by annealing to 1300−1400 K, to regain the crystalline structure. Thereafter, it was cleaned by cycles of O_2 thermal treatment at $p(O_2) = 1.0-2.0 \times 10^{-7}$ Torr and ∼1000 K for 2 min, followed by flashing the surface to ∼1500 K. The cleanliness of the substrate was monitored by AES. Carbon and oxygen, the primary surface contaminants, are readily removed by several cleaning cycles.

The 18 MΩ H_2O, pyridine (Fisher, certified A.C.S. grade, 99.9%), and perdeuterated pyridine (Aldrich Chemical Co., Inc., 99.96+ atom %D) were de-gassed by freeze, pump, and thaw cycles. The cleanliness of the gases introduced into the chamber was checked in situ by mass spectrometry.

Thin films of nonhydroxylated and hydroxylated γ-Al_2O_3, used throughout the experiments and characterized by AES and HREELS, were prepared by exposing the NiAl(100) substrate to O_2 or H_2O at 1000 K. In previous experiments, we have shown that Al_2O_3 films grown at 1000 K with an AES O(505)/Ni(848) ratio in the range of 2.5−3.0 show intense, narrow phonon structures indicative of high-quality, ordered films. This ratio was obtainable by either a 2400 L O_2 or a 100 L H_2O exposure (1 L = 1×10^{-6} Torr s). During preparation of

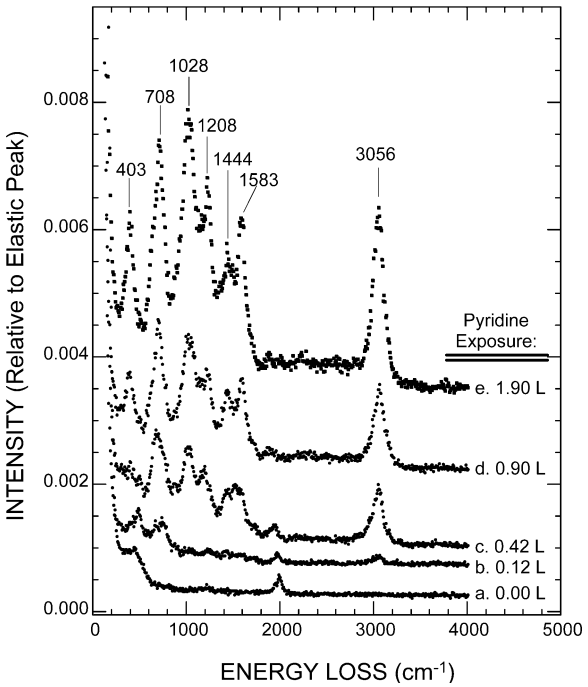

Figure 2. HREELS spectra depicting the coverage dependence for pyridine adsorption on NiAl(100) at 140 K. Pyridine exposures are as indicated for each spectrum.

γ-Al_2O_3 films for HREELS experiments, the background pressure in the chamber during the film growth did not exceed $p(O_2) = 2.0 \times 10^{-7}$ Torr and $p(H_2O) = 1.0 \times 10^{-8}$ Torr, respectively. In the HREELS chamber all exposures were corrected only for the doser flux enhancement of ×50. For the LITD-FTMS experiments, the oxide layer was grown at an oxygen exposure of 15 000 L at 930 K where the background oxygen pressure was 2.0×10^{-7} Torr. Hydroxylated surfaces were prepared by exposing the nonhydroxylated surface to 1 L of water at 300 K. Spectroscopically, these hydroxylated films are identical to the hydroxylated films grown in the HREELS chamber. In the LITD-FTMS chamber, all exposures were corrected only for a doser flux enhancement of ×100.

3. Results and Discussion

3.1. Pyridine Adsorption on NiAl(100). To provide appropriate background information, HREELS was used to study the adsorption of both pyridine and perdeuterated pyridine on the NiAl(100) substrate. Figures 2 and 3 depict the HREELS spectra collected following pyridine and perdeuterated pyridine adsorption, respectively, at 140 K for several pyridine/perdeuterated pyridine exposures. Figures 2a and 3a correspond to the clean NiAl(100) sample. In this spectrum there are weak vibrational modes at 455 and 2000 cm^{-1}, corresponding to the metal−CO stretch and the C−O stretch, respectively, due to background CO contamination. Comparing the intensity of the C−O stretch to the intensity of the C−O stretch after exposing

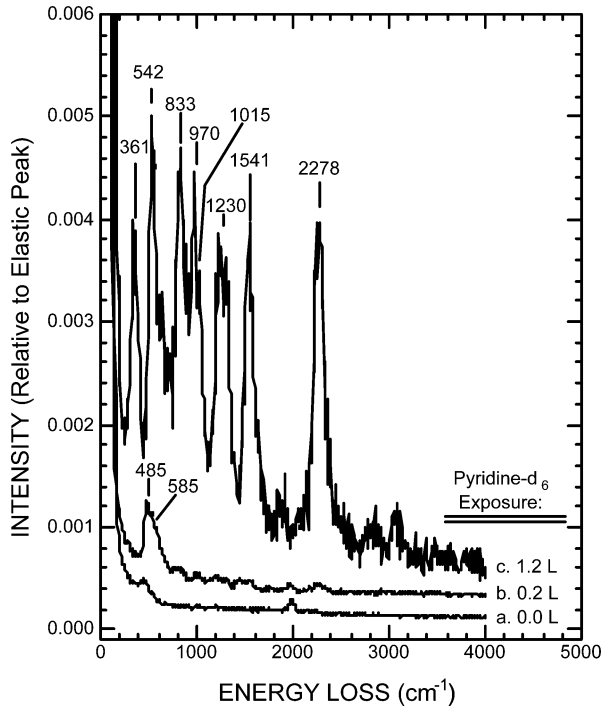

Figure 3. HREELS spectra collected after exposing the NiAl(100) surface to perdeuterated pyridine at 140 K. C_5D_5N exposures are as indicated for each spectrum.

the NiAl(100) to 0.1 L CO indicates that the CO contamination is less than 0.1 L.[70] After exposing the NiAl(100) crystal to 0.12 L pyridine (0.2 L perdeuterated pyridine), the strong vibrational modes in Figures 2b and 3b) are 403 (not observed for C_5D_5N), 495 (485), 665 (530), 750 (585) cm^{-1}, and 3056 (2278) cm^{-1} (energies of the perdeuterated pyridine modes are given in parentheses). These modes are, respectively, assigned to the out-of-plane ring distortion, metal−pyridine stretch, C−H (C−D) in-phase out-of-plane bend, the C−H (C−D) out-of-plane bend, and the C−H (C−D) stretch for the pyridine molecule.[71−75] According to the dipole scattering selection rules, the modes that we observe below 1000 cm^{-1} are dipole active when the pyridine molecule is bonded with its molecular plane parallel to the surface. The low intensity of the C−H (C−D) stretch at 3056 (2278) cm^{-1} further indicates that pyridine is oriented parallel to the NiAl(100) substrate, since the C−H (C−D) stretching modes in horizontally oriented adsorbates are generally weak.[71−75] In addition to the out-of-plane vibrational modes below 960 cm^{-1}, Figures 2b and 3b have very weak vibrational components between 960 and 1600 cm^{-1} due to the in-plane vibrations of pyridine. These in-plane vibrations are dipole active when the pyridine molecular axis is in a vertical or tilted orientation with respect to the surface plane.[71−75] On Ag(111), Demeuth et al.[74] observed that pyridine adsorbed parallel to the surface could undergo an additional interaction with the Ag(111) surface via the nitrogen-lone-pair orbital. This interaction caused a small inclination of the pyridine molecule on the Ag(111) surface.[76] We, therefore, propose that at low coverages, pyridine adsorbs parallel to the NiAl(100) surface, with a small inclination, by bonding through the π-orbitals with an additional surface interaction via the nitrogen-lone-pair electrons.

With increasing exposure (Figures 2c−e and 3c), marked changes in the HREELS spectra are observed. Primarily, the C−H (C−D) stretches at 3056 (2278) cm^{-1} and the energy loss modes between 960 and 1600 cm^{-1} (800−1550 cm^{-1}, in the case of perdeuterated pyridine) increase dramatically in intensity. For the adsorption of 1.9 L pyridine (1.2 L perdeuterated pyridine), these modes include an asymmetric ring breathing mode + C−H in-plane bend at 1028 (986) cm^{-1}, a C−H in-plane bend at 1208 (833) cm^{-1}, and C−C and C−N stretches at 1444 (1263) cm^{-1} and 1583 (1541) cm^{-1}.[71−75] In addition, the 403 (361) cm^{-1} energy-loss feature increases as the 495 (585) cm^{-1} loss decreases. The vibrations for the C−H out-of-plane bends at 665 (530) and 750 (585) cm^{-1} merge into a single C−H out-of-plane bend centered at 708 (542) cm^{-1}. These spectral changes indicate that pyridine adsorption undergoes an orientation transformation with increasing pyridine coverage. Specifically, the pyridine adsorbates tilt with the molecular plane toward the surface normal. These results are consistent with those reported in the literature for pyridine adsorption on Ag(111),[74] Pt(110),[77] Pt(111),[78] Ni(100),[75] Ni(110),[72] Ni(111),[71] and Cu(111).[73] Pyridine was observed to tilt between 55° and 75° from the surface plane on these metals. In fact, the observed vibrational modes for pyridine adsorbed on NiAl(100) are very similar to vibrational modes observed for pyridine on the Ni surfaces,[71,72,75] especially the Ni(110) substrate.[72] Table 2 summarizes the vibrational modes for pyridine adsorption on NiAl(100) and Ni(110) at both low and high pyridine coverages.

Further support that at high coverages, pyridine tilts toward the NiAl(100) surface normal is given in Figure 4. This figure depicts the vibrational spectra collected as a function of angular degrees from the specular direction after exposing the NiAl(100) substrate to 1.4 L pyridine at 140 K. In these spectra, the relative intensities of the vibrational modes at 403 and 708 cm^{-1} increase with respect to the other vibrational modes, suggesting that these modes have significant impact scattering contributions.[79] In addition, the C−H out-of-plane bend(s) at 708 cm^{-1} splits into two vibrational modes centered at 675 and 733 cm^{-1} with increasing degrees off the specular direction. The splitting of the C−H out-of-plane bends was observed for low pyridine coverages on the NiAl(100) substrate. The vibrational mode centered at 1208 cm^{-1}, due to an in-plane C−H bend, also has some impact character, but impact scattering is not as significant for this mode as it is for the out-of-plane vibrations. All other vibrational modes appear dipole active (i.e., the C−C, the C−N, and the C−H stretches). In summary, as coverage is increased, the primarily dipole scattered in-plane modes increase in intensity and the impact-scattered out-of-plane modes are still observed. Both of these observations provide support for the proposal that as the coverage is increased the molecular plane is inclined more toward the surface normal.

3.2. Pyridine Adsorption on Thin Films of γ-Al_2O_3/NiAl(100). The interaction of pyridine, as a function of coverage, on our nonhydroxylated and hydroxylated thin films of γ-Al_2O_3 at 170 K was studied using HREELS. Figure 5 depicts the HREELS spectra collected for the nonhydroxylated and hydroxylated γ-Al_2O_3 thin films after exposing them to a saturation coverage of pyridine at 170 K. Figure 5a is the spectrum of a freshly grown hydroxylated γ-Al_2O_3 thin film. While the γ-Al_2O_3 phonon modes hinder the observation of pyridine vibrations below 1100 cm^{-1}, the in-plane vibrations between 1100 and 1600 cm^{-1} are detectable. These in-plane vibrations, which are detectable on the γ-Al_2O_3 thin films even after pyridine exposures as small as 0.05 L, are observed over the background γ-Al_2O_3 combination and overtone bands, indicating that the molecular modes are quite intense. In addition, the C−H stretch is very intense. From these observations, we conclude that not surprisingly the pyridine molecules are interacting with the γ-Al_2O_3 thin films in a near vertical orientation through the

TABLE 2: Pyridine Mode Assignment on NiAl(100) and Ni(110)[a]

assignment	Ni(110) low exposure (cm^{-1})[b]	NiAl(100) low exposure (cm^{-1})	Ni(110) high exposure (cm^{-1})[b]	NiAl(100) high exposure (cm^{-1})
ring deformation	411/448	403 (not obs)	411/448	405 (361)
metal−pyridine stretch		495 (485)		
ring deformation	611		611	
C−H in phase out-of-plane bend	688	665 (520)	688	708 (542)
C−H out-of-plane bend	744	750 (585)	744	708 (542)
C−H out-of-plane bend	871		871	
asymmetric ring breathing + C−H in-plane bend			1016	1028 (986)
C−H in-plane bend			1209	1208 (833)
C−C + C−N stretch			1435	1444 (1263)
C−C + C−N stretch			1580	1583 (1541)
C−H stretch	3049	3056 (2263)	3049	3056 (2278)

[a] Mode energies in parentheses correspond to pyridine-d_5. [b] Ref 72.

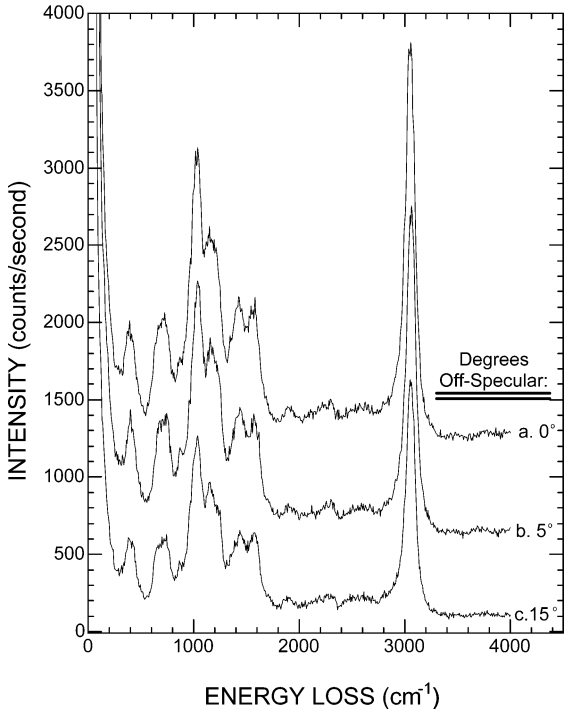

Figure 4. HREELS spectra for different scattering geometries following the adsorption of 1.4 L pyridine on the NiAl(100) substrate at 140 K. The angles indicate how many degrees the energy analyzer (scattered electron detector) was away from the specular scattering direction.

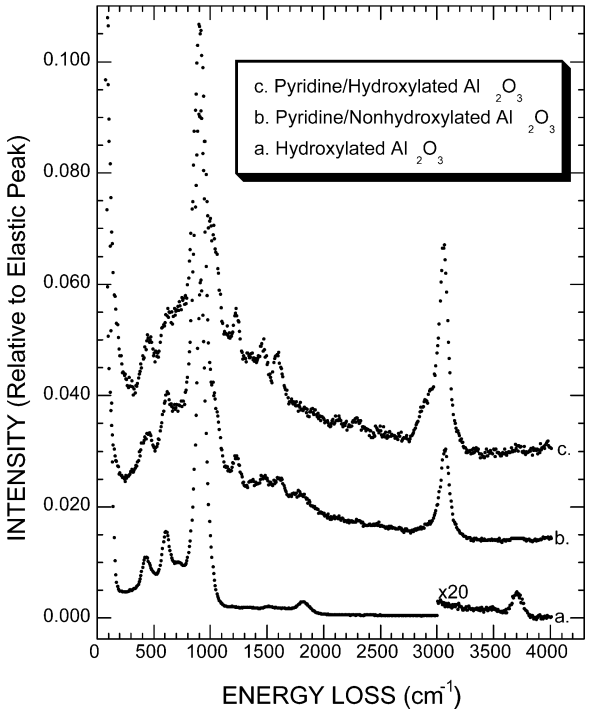

Figure 5. Comparison of the HREELS spectra collected for (a) hydroxylated γ-Al_2O_3 thin film, (b) a saturated pyridine coverage on nonhydroxylated γ-Al_2O_3 thin film, and (c) a saturated pyridine coverage on hydroxylated γ-Al_2O_3 thin film. Adsorption temperature was 170 K.

nitrogen-lone-pair electrons. Off-specular HREELS measurements support this conclusion; the observed in-plane pyridine vibrations are generally dipole active, although there may be a small contribution from impact scattering.

Since pyridine is interacting with the γ-Al_2O_3 thin film via its nitrogen-lone-pair electrons, and is oriented with the molecular plane approximately parallel to the surface normal, the frequencies of the pyridine ring vibrations should depend on the acidity and adsorption site for the pyridine molecules. Table 3 lists the observed vibrations between 1100 and 1600 cm^{-1} for pyridine adsorbed on the γ-Al_2O_3 thin films along with the typical vibrational frequencies for pyridine adsorbed on Brønsted acid, Lewis acid, and hydrogen-bonded sites. At our resolution, we can only use the $\bar{\nu}_{8a}$ mode at 1590−1600, 1640, or 1600−1633 cm^{-1} to distinguish between hydrogen-bonded, Brønsted acid, and Lewis acid interactions, respectively. The available Lewis acid sites on the nonhydroxylated γ-Al_2O_3 are very weak as indicated by the small blue-shift of the pyridine ring vibrations from the gas-phase values (Table 3). Since the expected ring vibrations for the potentially different binding sites are very close in frequency, we are unable to distinguish contributions from more than one adsorption site given the resolution of our HREELS spectrometer. However, we are able to make the observation that the frequency for the ring vibrations decreases when the molecule is adsorbed on the hydroxylated film, indicating that pyridine undergoes hydrogen bonding with the surface hydroxyl groups. The absence of ring vibrations at 1540 and 1620−1640 cm^{-1} indicates that these surface hydroxyl groups are not acting as strong Brønsted acid sites. Since it is evident that the nonhydroxylated γ-Al_2O_3 thin films have Lewis acids to which pyridine interacts, the hydroxylated γ-Al_2O_3 thin films should also have these Lewis acid sites. We therefore conclude that the observed frequencies for pyridine's ring vibrations on the thin films of hydroxylated γ-Al_2O_3 may be

TABLE 3: Vibrational Frequencies of Pyridine Adsorbed on Thin Films of γ-Al_2O_3

mode	hydrogen-bonded[a]	Brönsted acid[a]	Lewis acid[a]	non-hydroxylated	hydroxylated
$\bar{\upsilon}_{C-H}$	3087	3087	3087	3069	3059
$\bar{\upsilon}_{8a}$	1590−1600	1640	1600−1633	1613	1594
$\bar{\upsilon}_{8b}$	1580−1590	1620	1580		
$\bar{\upsilon}_{19a}$	1485−1490	1485−1500	1488−1503	1475	1456
$\bar{\upsilon}_{19b}$	1440−1447	1540	1447−1460		
$\bar{\upsilon}_{14}$	1362	1362	1362	1366	1366
$\bar{\upsilon}_{9a}$	1218	1218	1218	1225	1225

[a] Ref 38.

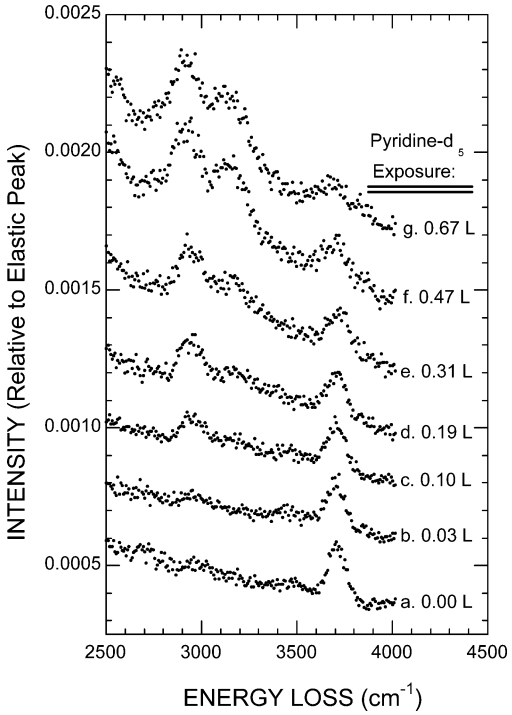

Figure 6. HREELS spectra depicting the coverage dependence for C_5D_5N−HO complex formation on the hydroxylated γ-Al_2O_3 thin film at 170 K. Only the OH stretch frequency region is shown for clarity. Perdeuterated pyridine (C_5D_5N) exposures are as indicated for each spectrum.

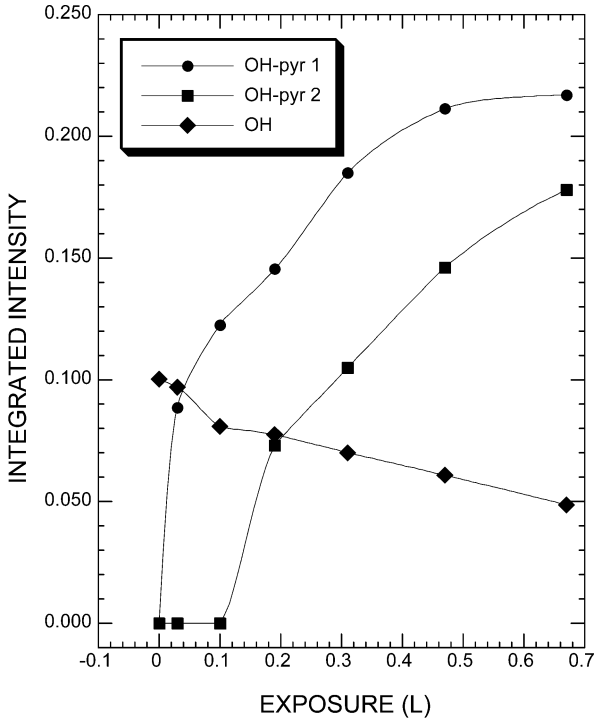

Figure 7. Integrated intensities for each of the three OH stretch modes shown in Figure 6, as a function of pyridine(d_5) exposure. The solid lines are guides to the eye only.

an average of pyridine interacting with the surface Lewis acid sites and hydrogen bonding to the surface hydroxyl groups.

Additional evidence that pyridine is hydrogen bonding on the hydroxylated γ-Al_2O_3 thin films includes the presence of a shoulder at ∼2920 cm^{-1} only on the hydroxylated thin films. The intensity of this shoulder, which has significant impact scattering character similar to the surface hydroxyl groups on the hydroxylated thin films, increases with increasing pyridine coverage as the intensity of the O−H stretch for the surface hydroxyl groups decreases. The interaction of pyridine with surface hydroxyl groups has been previously reported to shift the frequency of the "free" isolated O−H stretch to lower frequency.[35] Therefore, the vibration at ∼2920 cm^{-1} has been assigned to the pyridine−HO hydrogen bonded complex.

Figure 6, which depicts the O−H region for HREELS spectra collected after exposing the hydroxylated thin films of γ-Al_2O_3 to perdeuterated pyridine, confirms the assignment of the band at 2920 cm^{-1} to the O−H stretch for the pyridine(d_5)−OH complex. After exposing the hydroxylated thin films to 0.1 L perdeuterated pyridine at 170 K (Figure 6b), a pyridine(d_5)−OH complex is observed at 2920 cm^{-1}. The relative intensity increase and broadening of this vibrational mode compared to the free O−H stretch is further indication that this vibration is due to surface O−H groups hydrogen-bonded to pyridine(d_5); complexation of adsorbates with surface OH groups has previously been reported to increase the intensity, broaden the band, and red-shift the frequency of the isolated surface O−H groups.[35] The intensity of the isolated OH stretch at 3711 cm^{-1} has decreased. With increasing exposures of perdeuterated pyridine, the intensity of this pyridine(d_5)−HO complex vibration at 2920 cm^{-1} continues to increase as the intensity of the isolated O−H stretch continues to decrease. Interestingly, after exposing the hydroxylated thin film of γ-Al_2O_3 to 0.3 L perdeuterated pyridine, a second pyridine(d_5)−OH complex is observed at 3150 cm^{-1}. With further perdeuterated pyridine exposure, this band increases as the intensity for the O−H stretch continues to decrease. At this point, the intensity for the pyridine(d_5)−HO complex at 2920 cm^{-1} remains constant. The relative intensities of the three OH stretch vibrations are more easily seen in Figure 7, where we plot the integrated intensity of each mode as a function of pyridine exposure. Complex 1 (2920 cm^{-1}) grows in and saturates first, followed by the growth of intensity for complex 2 (3150 cm^{-1}) as the uncomplexed OH mode decreases in intensity.

The amount that the free O−H stretch is red-shifted on complexation with a probe base (e.g., pyridine) depends on the strength of the interaction; the stronger the interaction is, the more the O−H bond is weakened. The weakening of this O−H

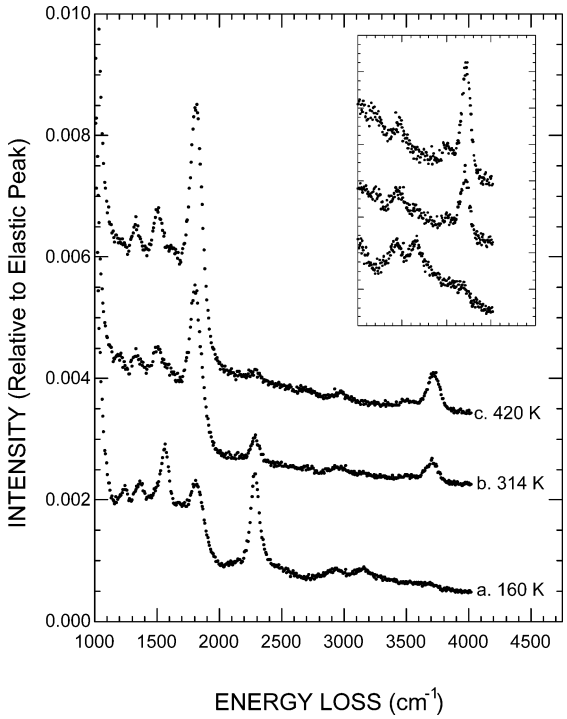

Figure 8. HREELS spectra depicting the adsorption of perdeuterated pyridine on the hydroxylated γ-Al_2O_3 thin films as a function of anneal temperature. For this experiment, a hydroxylated γ-Al_2O_3 thin film was exposed to 1.0 L perdeuterated pyridine at 160 K. The film was then annealed at the indicated temperature for ~5 s. All spectra were obtained after cooling the sample to 160 K.

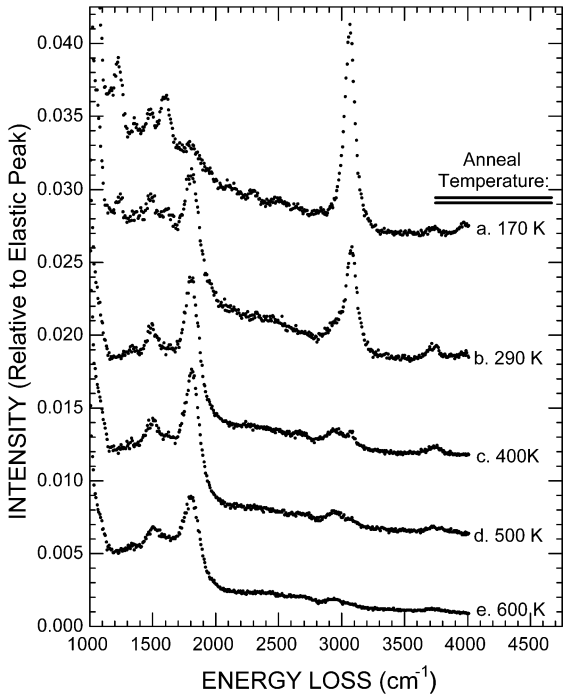

Figure 9. HREELS spectra depicting the adsorption of pyridine on the nonhydroxylated γ-Al_2O_3 thin films as a function of anneal temperature. For this experiment, a nonhydroxylated γ-Al_2O_3 thin film was exposed to 0.4 L pyridine at 170 K. The film was then annealed at the indicated temperatures for ~5 s. All spectra were obtained after cooling the sample to 170 K.

bond is responsible for the observed frequency shift for the O−H stretch of the complex. Since we observe two vibrations for the pyridine−HO complex, we conclude that we have two distinct surface OH groups differing in surface acidity. The shift for the O−H stretch is greater for the pyridine−HO complex at 2920 cm^{-1}. Thus, this is the complex of pyridine hydrogen bonding to the more acidic surface OH groups. This is consistent with the observation that this complex is formed at lower pyridine coverages than for the pyridine−HO complex resulting from pyridine interacting with the less acidic surface OH groups which grows in at higher coverage. As indicated previously, prior to pyridine adsorption, the OH stretch mode (3711 cm^{-1}) shows that the surface OH groups are bonded to 2 or 3 Al^{3+} cations and that there are no OH groups bonded to single Al^{3+} sites under our experimental conditions. Isolated surface OH groups bonded to 3 Al^{3+} cations are expected to be more acidic than isolated surface OH groups bonded to 2 Al^{3+} cations. We, therefore, assign the pyridine−HO complex at 2920 cm^{-1} to pyridine interacting with an OH group bonded to 3 Al^{3+} cations and the pyridine−HO complex at 3150 cm^{-1} to pyridine interacting with an OH group bonded to 2 Al^{3+} cations.

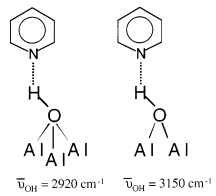

3.3. Pyridine Desorption from Thin Films of γ-Al_2O_3/NiAl-(100). Desorption of pyridine (perdeuterated pyridine) from the hydroxylated and nonhydroxylated thin films was studied using HREELS and laser-induced thermal desorption coupled with Fourier transform mass spectrometry (LITD-FTMS). Figure 8 depicts the HREELS spectra collected after annealing a hydroxylated thin film of γ-Al_2O_3 previously exposed to 1.0 L perdeuterated pyridine at 160 K (Figure 8a). The inset of this figure magnifies the O−H stretching region, showing the vibrations of the two pyridine−HO complexes. After annealing to 314 K (Figure 8b), pyridine is completely removed from the less acidic surface OH groups. This is indicated by the decrease in the intensity of the O−H stretch for the pyridine−HO complex at 3150 cm^{-1}. While the intensity of the O−H stretch for the pyridine−HO complex at 2920 cm^{-1} is also substantially reduced, pyridine is not completely removed from the more acidic surface OH groups until after annealing the film to 420 K (Figure 8c). As the intensities of the O−H stretch for the pyridine−HO complexes at 2920 and 3150 cm^{-1} decrease, the intensity for the "free" O−H stretch at 3711 cm^{-1} increases. This observation further confirms the assignment of the vibrational modes at 2920 and 3150 cm^{-1} as the O−H stretches for the pyridine−HO complexes formed when pyridine interacts with the more acidic and less acidic surface OH groups, respectively.

Likewise, the HREELS spectra collected after annealing a nonhydroxylated thin film of γ-Al_2O_3 previously exposed to 0.4 L pyridine at 170 K (Figure 9) indicate that most of the pyridine is removed after annealing to 400 K (Figure 9c). Interestingly, after annealing to 290 K (Figure 9b), a small fraction of the pyridine on the nonhydroxylated thin films dehydrogenates forming a small amount of surface OH and presumably hydrocarbon fragments as indicated by the OH stretch at 3742 cm^{-1}. In addition, a shoulder is observed at approximately 2920 cm^{-1}, indicating that some of the remaining pyridine is interacting with these newly formed surface OH groups. After annealing to 400 K (Figure 9c), most of the pyridine and/or pyridine fragments remaining on the surface

are interacting with surface OH groups formed from the dehydrogenation of pyridine on the nonhydroxylated thin films of γ-Al_2O_3. LITD-FTMS experiments support the observation that a small amount of the pyridine dehydrogenates on the nonhydroxylated thin films of γ-Al_2O_3. In these experiments, the nonhydroxylated thin films of γ-Al_2O_3 were exposed to 40 L pyridine at 140 K. Then, the sample was annealed to ~300 K at ~20 K increments. A LITD-FTMS spectrum was collected while maintaining the substrate temperature at each of these increments. After annealing the nonhydroxylated thin films to 295 K, the ions corresponding to pyridine are no longer detectable in the LITD-FTMS spectra. The absence of laser desorption of molecular pyridine at temperatures above 300 K, yet the presence of C−H stretches in the HREELS spectra for anneal temperatures ~ 400 K, is indicative that a small amount of pyridine is dehydrogenating on these surfaces. This is not unexpected since pyridine dehydrogenation has been observed on several catalytic surfaces including Ni(111),[71] Ni(110),[72] Ni-(100),[75] and Pt(111).[80] In these systems, the dehydrogenation results in the formation of an α-pyridinyl species. Cleavage of the C−H bond and OH formation has also been observed for hydrocarbons, such as 1,3-butadiene on the γ-Al_2O_3 surfaces.[32,33]

Dehydrogenation is also observed on the hydroxylated thin film of γ-Al_2O_3. There appear to be more surface OH groups on these films as indicated by an interacting O−H stretch at 3508 cm^{-1}(Figure 8b,c). This implies that the surface OH concentration has increased so that OH groups are interacting with each other. Support for the dehydrogenation on the hydroxylated surfaces was observed in the LITD-FTMS experiments as well. Following a 40 L pyridine exposure to a hydroxylated γ-Al_2O_3 thin film, the ions corresponding to pyridine ($m/z = 50$ and $m/z = 79$) are no longer detected after annealing the hydroxylated γ-Al_2O_3 film to 275 K. A small amount of dedeuteration is also seen after annealing perdeuterated pyridine on the hydroxylated thin films to temperatures ≥ 314 K as indicated by an O−D stretch at 2722 cm^{-1} (Figure 8b). From these results, we conclude that although the formation of the pyridine−HO complexes is mostly reversible, a small amount of pyridine dehydrogenates on the γ-Al_2O_3 thin films.

4. Summary

The adsorption of pyridine on NiAl(100) and the nonhydroxylated and hydroxylated thin films of γ-Al_2O_3 was investigated using high-resolution electron energy loss spectroscopy (HREELS). On NiAl(100), the adsorption orientation of pyridine is coverage dependent. At low coverages, pyridine adsorbs with its molecular plane parallel to the NiAl(100) surface. As the coverage is increased, the molecular plane tilts toward the surface normal. This behavior is similar to that seen previously on other transition-metal surfaces.

Pyridine adsorbs on the nonhydroxylated and hydroxylated Al_2O_3 ultrathin films with its molecular plane tilted toward the surface normal via the nitrogen-lone-pair electrons interacting with the surface Lewis acid sites and hydrogen-bonding with the surface OH groups, respectively. While the pyridine interaction with the Lewis acid sites is partially irreversible, the pyridine interaction with the surface OH is reversible. Therefore, pyridine should be a good probe for quantitatively determining the surface OH acidity. When pyridine hydrogen bonds to a surface OH group, the O−H bond is weakened, causing a red shift in the O−H stretch frequency. We observe the formation of two distinct pyridine−HO complexes on thin films of hydroxylated γ-Al_2O_3. This result is indicative that we have two distinct surface hydroxyl groups. Since the degree that the O−H stretching frequency is shifted depends on the interaction strength, this shift can be used to determine the relative surface acidity of the two types of surface OH species. We have assigned the pyridine−HO complex with an OH stretch mode at 2920 cm^{-1} to be due to pyridine interacting with the more acidic surface OH groups, specifically, those in which the surface OH is bonded to 3 Al^{3+} cations. The pyridine−HO complex with an OH stretch mode at 3150 cm^{-1} is assigned to pyridine interacting with the less acidic surface OH groups, specifically, those in which the surface OH is bonded to 2 Al^{3+} cations. The shift in the OH stretching frequency on complex formation is related to the interaction strength, which depends on both the acidity of the OH group and the basicity of the probe molecule (pyridine in these studies). If we can study these complexation-related frequency shifts for a number of probe molecules of differing and known basicity, we should be able to separate the effects of probe basicity and OH acidity and thus directly determine the OH acidity. This will be the subject of a subsequent manuscript.

Acknowledgment. This work was supported by the National Science Foundation under Grant CHE-9819399. The authors thank H. J. Freund and M. Baumer for numerous discussions about the results presented in this manuscript.

References and Notes

(1) Corado, A.; Kiss, A.; Knozinger, H.; Muller, H.-D. *J. Catal.* **1975**, *37*, 68.
(2) Hightower, J. W.; Hall, W. K. *J. Catal.* **1969**, *13*, 161.
(3) Hightower, J. W.; Hall, W. K. *Trans. Faraday Soc.* **1970**, *66*, 477.
(4) Knozinger, H.; Ratnasamy, P. *Catal. Rev.-Sci. Eng.* **1978**, *17*, 31.
(5) MacIver, D. S.; Wilmot, W. H.; Bridges, J. M. *J. Catal.* **1964**, *3*, 502.
(6) Medema, J. *J. Catal.* **1975**, *37*, 91.
(7) deVries, J. E.; Yao, H. C.; Baird, R. J.; Gandhi, H. S. *J. Catal.* **1983**, *84*, 8.
(8) Furlong, B. K.; Hightower, J. W.; Chan, T. Y.-L.; Sarkany, A.; Guczi, L. *Appl. Catal. A* **1994**, *117*, 41.
(9) Kaushik, V. K.; Sivaraj, C.; Rao, P. K. *Appl. Surf. Sci.* **1991**, *51*, 27.
(10) Coster, D. J. *Langmuir* **1995**, *11*, 2615.
(11) Gassmann, P.; Franchy, R.; Ibach, H. *Surf. Sci.* **1994**, *319*, 95.
(12) Saniger, J. M. *Mater. Lett.* **1995**, *22*, 109.
(13) Knozinger, H. *Adv. Catal.* **1976**, *25*, 184.
(14) Morterra, C.; Magnacca, G. *Catal. Today* **1996**, *27*, 497.
(15) Baumgarten, E.; Wagner, R.; Lentes-Wagner, C. *Fresenius' Z. Anal. Chem.* **1989**, *334*, 246.
(16) Wu, Y.; Grfunkel, E.; Madey, T. *J. Vac. Sci. Technol. A* **1996**, *14*, 2554.
(17) Chen, J. G.; Crowell, J. E.; Yates, J. T., Jr. *J. Chem. Phys.* **1986**, *84*, 5906.
(18) Chen, J. G.; Crowell, J. E.; Yates, J. T., Jr. *Phys. Rev. B* **1986**, *33*, 1436.
(19) Chen, P. J.; Colaianni, M. L.; Yates, J. T., Jr. *Phys. Rev. B* **1990**, *41*, 8025.
(20) Chen, P. J.; Goodman, D. W. *Surf. Sci.* **1994**, *312*, L767.
(21) Crowell, J. E.; Chen, J. G.; Yates, J. T., Jr. *Surf. Sci.* **1986**, *165*, 37.
(22) Wu, Y.; Garfunkel, E.; Madey, T. *Surf. Sci.* **1996**, *365*, 337.
(23) Wu, M.-C.; Goodman, D. W. *J. Phys. Chem.* **1994**, *98*, 9871.
(24) Becker, C.; Kandler, J.; Raaf, H.; Linke, R.; Pelster, T.; Drager, M.; Tanemura, M. *J. Vac. Sci. Technol. A* **1998**, *16*, 1000.
(25) Blum, R.-P.; Niehus, H. *Appl. Phys. A* **1998**, *66*, S529.
(26) Gassmann, P.; Franchy, R.; Ibach, H. *J. Electron Spectrosc. Relat. Phenom.* **1993**, *64−65*, 315.
(27) Baumer, M.; Freund, H.-J. *Prog. Surf. Sci.* **1999**, *61*, 127.
(28) Jaeger, R. M.; Kuhlenbeck, H.; Freund, H.-J.; Wuttig, M.; Hoffmann, W.; Franchy, R.; Ibach, H. *Surf. Sci.* **1991**, *259*, 235.
(29) Libuda, J.; Frank, M.; Sandell, A.; Anderson, S.; Bruhwiler, P. A.; Baumer, M.; Martensson, N.; Freund, H.-J. *Surf. Sci.* **1997**, *384*.
(30) Libuda, J.; Winklemann, F.; Baumer, M.; Freund, H.-J.; Bertrams, T.; Neddermeyer, H.; Muller, K. *Surf. Sci.* **1994**, *318*, 61.

(31) Franchy, R.; Masuch, J.; Gassmann, P. *Appl. Surf. Sci.* **1996**, *93*, 317.
(32) Ivey, M. M.; Allen, H. C.; Avoyan, A.; Martin, K. A.; Hemminger, J. C. *J. Am. Chem. Soc.* **1998**, *120*, 10980.
(33) Ivey, M. M.; Layman, K. A.; Avoyan, A.; Allen, H. C.; Hemminger, J. C. *J. Phys. Chem.* **2003**, *107*, 6391.
(34) Ballinger, T. H.; Yates, J. T., Jr. *Langmuir* **1991**, *7*, 3041.
(35) Lercher, J. A.; Grundling, C.; Eder-Mirth, G. *Catal. Today* **1996**, *27*, 353.
(36) Heemeier, M.; Frank, M.; Libuda, J.; Wolter, K.; Kuhlenbeck, H.; Baumer, M.; Freund, H.-J. *Catal. Lett.* **2000**, *68*, 19.
(37) Morterra, C.; Cerrato, G. *Catal. Lett.* **1991**, *10*, 357.
(38) Ferwerda, R.; van der Maas, J. H.; van Duijneveldt, F. B. *J. Mol. Catal. A* **1996**, *104*, 319.
(39) Hatayama, F.; Ohno, T.; Maruoka, T.; Ono, T.; Miyata, H. *J. Chem. Soc. Faraday Trans.* **1991**, *87*, 2629.
(40) Hess, A.; Kemnitz, E. *J. Catal.* **1994**, *149*, 449.
(41) Wilson, E. B. *Phys. Rev.* **1934**, *45*, 706.
(42) Kijenski, J.; Baiker, A. *Catal. Today* **1989**, *5*, 1.
(43) Amster, I. J.; Land, D. P.; Hemminger, J. C.; McIver, R. T., Jr. *Anal. Chem.* **1989**, *61*, 184.
(44) Amster, I. J.; Land, D. P.; Hemminger, J. C.; McIver, R. T., Jr. *Adv. Mass Spectrosc.* **1989**, *11*, 680.
(45) Behm, J. M.; Hemminger, J. C.; Lykke, K. R. *Anal. Chem.* **1996**, *68*, 713.
(46) Hemminger, J. C. In *Laser Spectroscopy and Photochemistry on Metal Surfaces, Part I*; Dai, H.-L., Ho, W., Eds.; World Scientific: Singapore, 1995; Vol. 5, Chapter 7.
(47) Huang, J.; Hemminger, J. C. *J. Am. Chem. Soc.* **1993**, *115*, 3342.
(48) Huang, J.; Tiedemann, P. W.; Land, D. P.; McIver, R. T., Jr.; Hemminger, J. C. *Int. J. Mass Spectrosc.* **1994**, *134*, 11.
(49) Land, D. P.; Tai, T.-L.; Lindquist, J. M.; Hemminger, J. C.; McIver, R. T., Jr. *Anal. Chem.* **1987**, *59*, 2924.
(50) Land, D. P.; Tai, T.-L.; Lindquist, J. M.; Hemminger, J. C.; McIver, R. T., Jr. *J. Vac. Sci. Technol. A* **1988**, *6*, 1024.
(51) Land, D. P.; Pettiette-Hall, C. L.; McIver, R. T., Jr.; Hemminger, J. C. *J. Am. Chem. Soc.* **1989**, *111*, 5970.
(52) Land, D. P.; Wang, D. T. S.; Tai, T.-L.; Sherman, M. G.; Hemminger, J. C.; McIver, R. T., Jr. In *Lasers and Mass Spectrometry*; Lubman, D. M., Ed.; Oxford University Press: New York, 1990; Chapter 7, p 157.
(53) Land, D. P.; Pettiette-Hall, C. L.; Sander, D.; McIver, R. T., Jr.; Hemminger, J. C. *Rev. Sci. Instrum.* **1990**, *61*, 1674.
(54) Land, D. P.; Pettiette-Hall, C. L.; Hemminger, J. C.; McIver, R. T., Jr. *Acc. Chem. Res.* **1991**, *24*, 42.
(55) Li, Y.; McIver, R. T., Jr.; Hemminger, J. C. *J. Chem. Phys.* **1990**, *93*, 4719.
(56) Li, Y.; Huang, J.; McIver, R. T., Jr.; Hemminger, J. C. *J. Am. Chem. Soc.* **1992**, *114*, 2428.
(57) McIver, R. T., Jr.; Sherman, M. G.; Land, D. P.; Kingsley, J. R.; Hemminger, J. C. In *Secondary Ion Mass Spectrometry, SIMS V*; Benninghoven, A., Colton, R. J., Simons, D. S., Werner, H. W., Eds.; Springer-Verlag: New York, 1986.
(58) Pansoy-Hjelvik, M. E.; Schnabel, P.; Hemminger, J. C. *J. Phys. Chem. B* **2000**, *104*, 6554.
(59) Parker, D. H.; Wurtz, P.; Chatterjee, K.; Lykke, K. R.; Hunt, J. E.; Pellin, M. J.; Hemminger, J. C.; Gruen, D. M.; Stock, L. M. *J. Am. Chem. Soc.* **1991**, *113*, 7499.
(60) Parker, D. H.; Pettiette-Hall, C. L.; Li, Y.; McIver, R. T., Jr.; Hemminger, J. C. *J. Phys. Chem.* **1992**, *96*, 1888.
(61) Parker, D. H.; Chatterjee, K.; Wurtz, P.; Lykke, K. R.; Pellin, M. J.; Stock, L. M.; Hemminger, J. C. *Carbon* **1992**, *30*, 1167.
(62) Pettiette-Hall, C. L.; Land, D. P.; McIver, R. T., Jr.; Hemminger, J. C. *J. Phys. Chem.* **1990**, *94*, 1948.
(63) Pettiette-Hall, C. L.; Land, D. P.; McIver, R. T., Jr.; Hemminger, J. C. *J. Am. Chem. Soc.* **1991**, *113*, 2755.
(64) Sherman, M. G.; Kingsley, J. R.; Dahlgren, D. A.; Hemminger, J. C.; McIver, R. T., Jr. *Surf. Sci.* **1985**, *148*, L25.
(65) Sherman, M. G.; Kingsley, J. R.; McIver, R. T., Jr.; Hemminger, J. C. *ACS Symp. Ser.* **1985**, *288*, 238.
(66) Sherman, M. G.; Kingsley, J. R.; Hemminger, J. C.; McIver, R. T., Jr. *Anal. Chim. Acta* **1985**, *178*, 79.
(67) Sherman, M. G.; Land, D. P.; McIver, R. T., Jr.; Hemminger, J. C. *J. Vac. Sci. Technol. A* **1986**, *4*, 1507.
(68) Sherman, M. G.; Land, D. P.; Hemminger, J. C.; McIver, R. T., Jr. *Chem. Phys. Lett.* **1987**, *137*, 298.
(69) Burgess, D., Jr.; Viswanathan, R.; Hussla, I.; Stair, P. C.; Weitz, E. *J. Chem. Phys.* **1983**, *79*, 5200.
(70) Jiang, Y.; Hemminger, J. C. Personal communication, 2002.
(71) Cohen, M. R.; Merrill, R. P. *Langmuir* **1990**, *6*, 1282.
(72) Cohen, M. R.; Merrill, R. P. *Surf. Sci.* **1991**, *245*, 1.
(73) Davies, P. R.; Shukla, N. *Surf. Sci.* **1995**, *322*, 8.
(74) Demuth, J. E.; Christmann, K.; Sanda, P. N. *Chem. Phys. Lett.* **1980**, *76*, 201.
(75) DiNardo, N. J.; Avouris, P.; Demuth, J. E. *J. Chem. Phys.* **1984**, *81*, 2169.
(76) Gassmann, P.; Schmitz, G.; Boysen, J.; Batolucci, F.; Franchy, R. *J. Vac. Sci. Technol. A* **1996**, *14*, 813.
(77) Surman, M.; Bare, S. R.; Hofmann, P.; King, D. A. *Surf. Sci.* **1987**, *179*, 243.
(78) Kahn, B. E.; Chaffins, S. A.; Gui, J. Y.; Lu, F.; Stern, D. A.; Hubbard, A. T. *Chem. Phys.* **1990**, *141*, 21.
(79) Ibach, H.; Mills, D. L. *Electron Energy Loss Spectroscopy and Surface Vibrations*; Academic Press: New York, 1982.
(80) Wexler, R. M.; Tsai, M.-C.; Friend, C. M.; Muetterties, E. L. *J. Am. Chem. Soc.* **1982**, *104*, 2034.
(81) Wiberg, K. B.; Walters, V. A.; Wong, K. N.; Colson, S. T. *J. Phys. Chem.* **1984**, *88*, 6067.